

- Achievement of hearing preservation in the presence of an electrode covering the residual hearing region、耳科コレギウム国際学会、ハンガリー (2010年8月)
- 9) 宇佐美真一、工 穰、鈴木伸嘉、茂木英明、宮川麻衣子、西尾信哉、残存聴力活用型人工内耳 (EAS:electric acoustic stimulation) :手術法と聴力保存成績について、第 20 会日本耳科学会総会、愛媛 (2010年10月)
- 10) 宮川麻衣子、我妻道生、西尾信哉、宇佐美真一、CDH23 遺伝子変異による難聴一変異解析と臨床像一、第 20 会日本耳科学会総会、愛媛 (2010年10月)
- 11) 内藤武彦、宮川麻衣子、西尾信哉、宇佐美真一、佐藤宏昭、熊川孝三、古屋信彦、東野哲也、優性遺伝形式をとる遺伝性難聴に関する実態調査と臨床像、愛媛 (2010年10月)
- 12) 宇佐美真一、遺伝性難聴、日本人類遺伝学会、大宮 (2010年10月)
- 13) 工 穰、茂木英明、塚田景太、宮川麻衣子、鬼頭良輔、宇佐美真一、GJB2 遺伝子変異症例における ASSR での推定聴力閾値と成長後の純音聴力検査閾値比較、第 55 回日本聴覚医学会総会・学術講演会、奈良 (2010年11月)
- 14) 鈴木宏明、福岡久邦、塚田景太、宇佐美真一、SLC26A4 遺伝子変異における平衡機能評価、第 69 回日本めまい平衡医学会総会、京都 (2010年11月)
- 15) 宇佐美真一、西尾信哉、工穰、茂木英明、菊池景子、古庄知己、福島義光、阿部聡子、長野誠、山口敏和「難聴の遺伝学的検査と遺伝カウンセリングに関する全国共同研究」第 53 回日本人類遺伝学会 (横浜)
- 16) 宇佐美真一、工穰、茂木英明、鬼頭良輔、菊池景子、西尾信哉「難聴の遺伝子検査と遺伝カウンセリングの全国共同研究:変異の検出頻度と患者アンケート調査について」第 53 回日本聴覚医学会総会・学術講演会 (東京)
- 17) 茂木英明、鬼頭良輔、菊池景子、工穰、宇佐美真一、内藤泰、前田麻貴、北野庸子「遺伝子と脳機能が評価できた先天性難聴症例」第 53 回日本聴覚医学会総会・学術講演会 (東京)
- 18) 茂木英明、塚田景大、橋本繁成、工穰、宇佐美真一「日本人難聴患者に見出された *TECTA* 遺伝子変異についての検討」第 18 回日本耳科学会総会・学術講演会 (神戸)
- 19) 林景子、塚田景大、工穰、新川秀一、南場淳司、熊川孝三、岩崎聡、高橋晴雄、神田幸彦、宇佐美真一「人工内耳患者の遺伝的背景についての検討」第 18 回日本耳科学会総会・学術講演会 (神戸)
- 20) 塚田景大、菊池景子、工穰、宇佐美真一「1500 家系 (3000 例) の難聴患者における *GJB2* 遺伝子解析—新規変異と臨床型について—」第 18 回日本耳科学会総会・学術講演会 (神戸)
- 21) 宇佐美真一、工穰、茂木英明、菊池景子「日本人難聴遺伝子データベースの構築:日本人に見出される変異と臨床応用について」第 18 回日本耳科学会総会・学術講演会 (神戸)
- 22) 福岡久邦、工穰、古舘佐起子、塚田景大、小口智啓、杉浦真、宇佐美真一「メニエール病におけるガドリニウム鼓室内投

- 与を用いた診断の有用性についての検討(第2報)」第67回日本めまい平衡医学会総会・学術講演会(秋田)
- 23) 塚田景大、福岡久邦、古籔佐起子、宮川麻衣子、工 穰、宇佐美真一「遺伝性難聴患者における前庭機能評価について」第67回日本めまい平衡医学会総会・学術講演会(秋24) 菊池景子、塚田景大、長井今日子、宇佐美真一、難聴患者におけるプレスチン遺伝子の変異解析、日本耳鼻咽喉科学会総会・学術講演会、東京(2009年5月)
- 25) 宇佐美真一、遺伝性難聴の診断と取り扱い、第71回耳鼻咽喉科臨床学会、旭川(2009年7月)
- 26) 古籔佐起子、茂木英明、鬼頭良輔、菊池景子、工 穰、宇佐美真一、人工内耳埋め込み術を行った無症候性先天サイトメガロウイルス-難聴児の2症例-、第71回耳鼻咽喉科臨床学会、旭川(2009年7月)
- 27) 宇佐美真一、難聴の遺伝子診断、日本人類遺伝学会第54回大会、東京(2009年9月)
- 28) 宇佐美真一、鈴木伸嘉、茂木英明、工 穰、人工内耳手術における残存聴力保存の試み、第19回日本耳科学会総会学術講演会、東京(2009.10月)
- 29) 橋本繁成、鈴木伸嘉、西尾信哉、宇佐美真一、新規難聴候補遺伝子ATPase, Na⁺/K⁺transporting, alpha2(+) polypeptide(ATP1A2)変異の機能解析、第19回日本耳科学会総会学術講演会、東京(2009.10月)
- 30) 古籔佐起子、茂木英明、西尾信哉、工 穰、宇佐美真一、小児感音難聴における無症候性先天性サイトメガロウイルス感染の関与について、第19回日本耳科学会総会学術講演会、東京(2009.10月)
- 31) 塚田景大、鈴木宏明、工 穰、宇佐美真一、両側進行性感音難聴患者における遺伝的背景についての検討、第54回日本聴覚医学会総会学術講演会、横浜(2009年10月)
- 32) 宮川麻衣子、鈴木伸嘉、茂木英明、工 穰、宇佐美真一、高音急墜型/高音漸傾型感音難聴症例の臨床像と遺伝的背景、第54回日本聴覚医学会総会学術講演会、横浜(2009年33) 北野庸子、宇佐美真一、工 穰、茂木英明、鈴木美華、前田麻貴、信州大学病院人工内耳センターにおける早期ハビリテーション-前言語聴覚学習プログラムの実施とその評価-、第54回日本聴覚医学会総会学術講演会、横浜(2009年10月)
- 34) 鈴木美華、茂木英明、工 穰、宇佐美真一、内藤泰、前田麻貴、北野庸子、遺伝子と脳機能が評価できた人工内耳装用児のコミュニケーション行動と発生の変化、第54回日本聴覚医学会総会学術講演会、横浜(2009年10月)
- 35) 茂木英明、古籔佐起子、鬼頭良輔、工 穰、宇佐美真一、小児一側性難聴120例の検討、第54回日本聴覚医学会総会学術講演会、横浜(2009年10月)
- 36) 宇佐美真一、難聴の遺伝子診断の現況、第1回難聴遺伝子の研究会、横浜(2009年10月)、第54回日本聴覚医学会総会学術講演会、横浜(2009年10月)
- H. 知的財産権の出願・登録状況
1. 特許取得

なし

2. 実用新案登録

なし

3. その他

なし

図1 *GJB2* 遺伝子変異の種類による難聴の程度 (Tsukada et al 2010 より)

1515 名の大規模解析により、遺伝子変異の種類 (組み合わせ) により難聴の程度が異なる事を明らかにした。(赤線が難聴患者全体の平均値、網掛は標準偏差を表す)

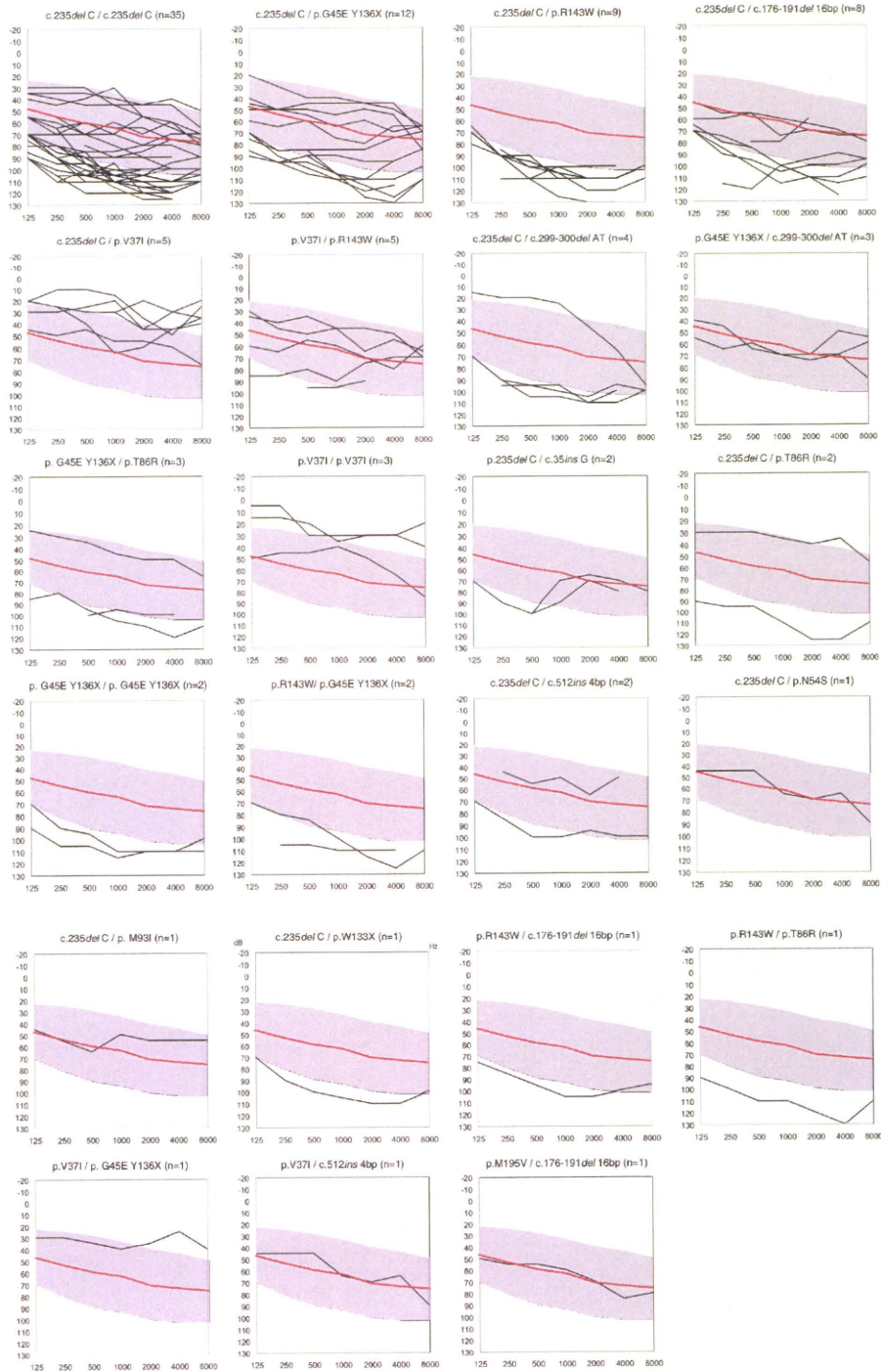


図2 難聴発見時の年齢と GJB2 遺伝子変異の種類 (Tsukada et al., 2010 より)

235delC 変異では難聴が高度となるため、言語取得前の発見が大部分であるのに対して、V37I 変異では難聴が軽度であるため難聴の発見が遅れる傾向にある。

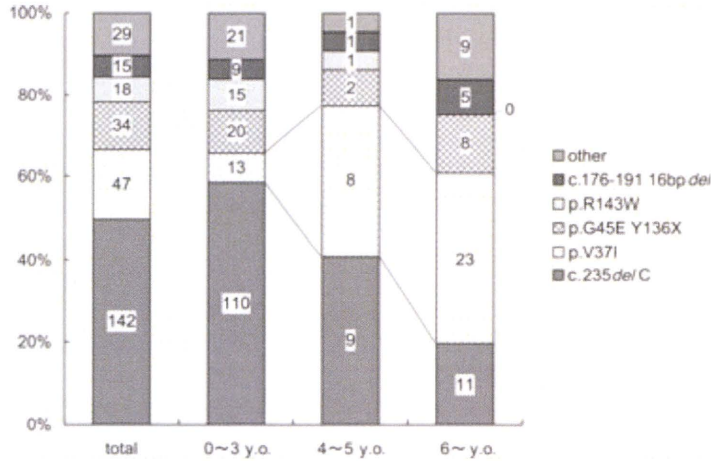


図3 ミトコンドリア 1555A>G 変異による難聴 (Lu et al., 2009 より)

(a) ミトコンドリア 1555A>G 変異を持つ患者では、年齢によらずおおよそ 20dB 聴力の悪化が認められる。(b) アミノ配糖体投与群では年齢と関係なく高度の難聴となる。

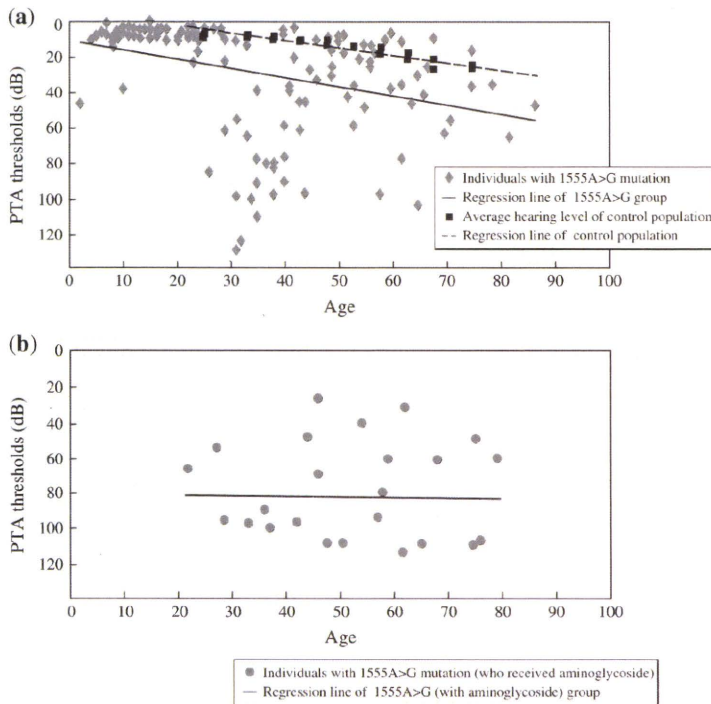


図3 高音急墜型の聴力像を呈する難聴患者の遺伝形式
 (Usami et al., 2010 より改変)

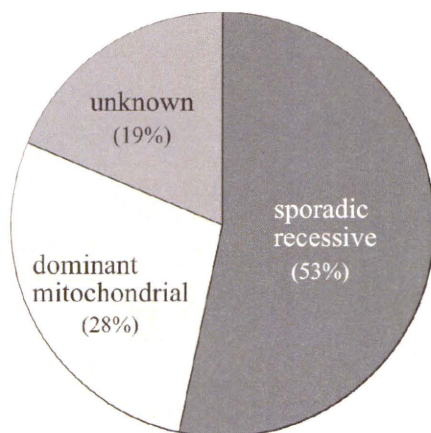


図4 難聴患者全体 (2587 例) と高音急墜型の聴力像を呈する難聴患者 (139 例) の進行性の比較 (Usami et al., 2010 より改変)

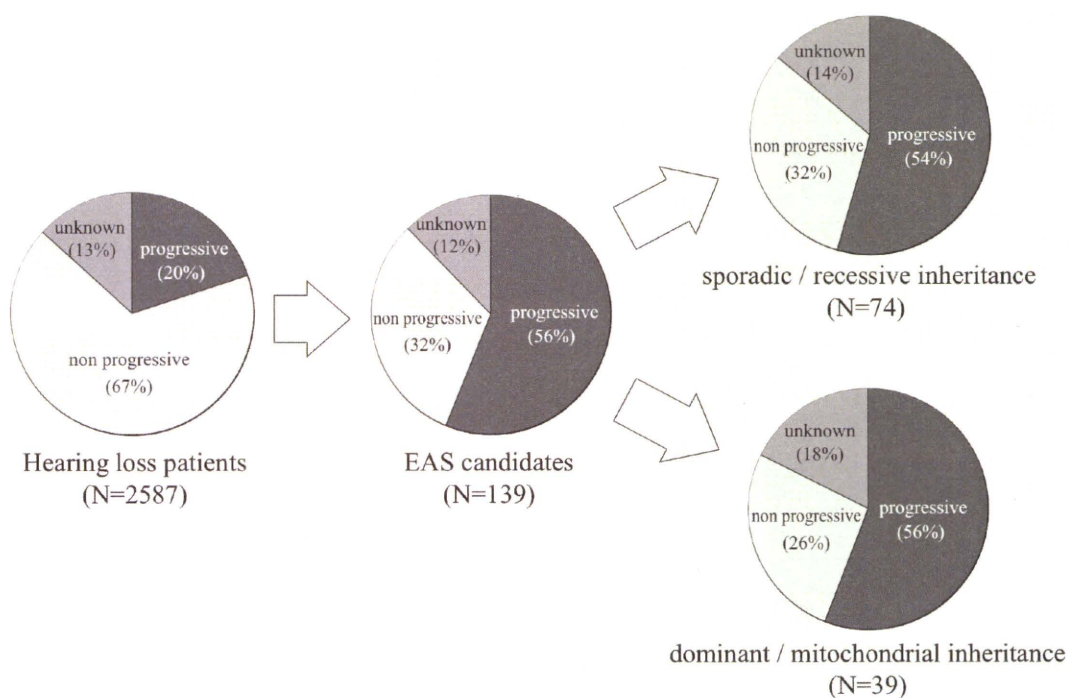


図5 遺伝形式別に見た高音急墜型の聴力像を呈する難聴患者の発症年齢
(難聴診断時年齢) (Usami et al., 2010 より改変)

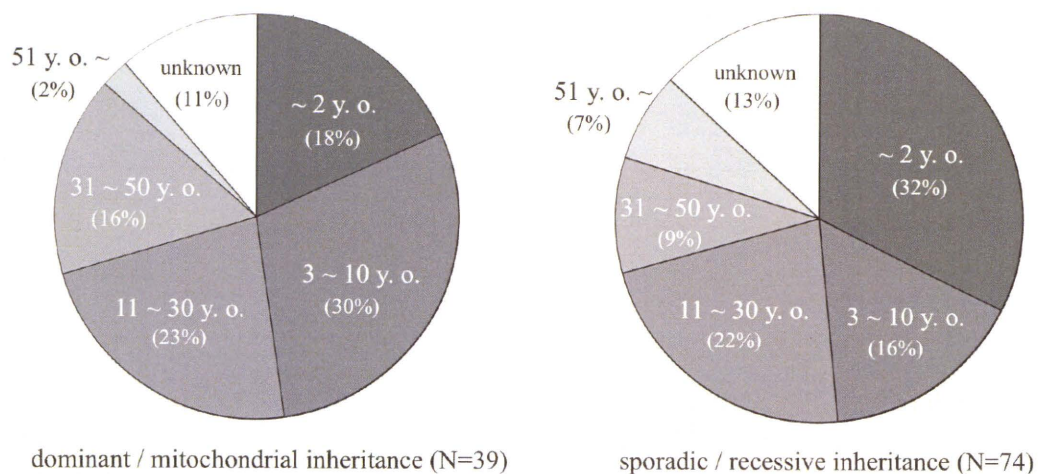


図6 遺伝形式別に見た高音急墜型の聴力像を呈する難聴患者 (139例) に認められる
難聴原因遺伝子変異の種類と割合 (Usami et al., 2010 より改変)

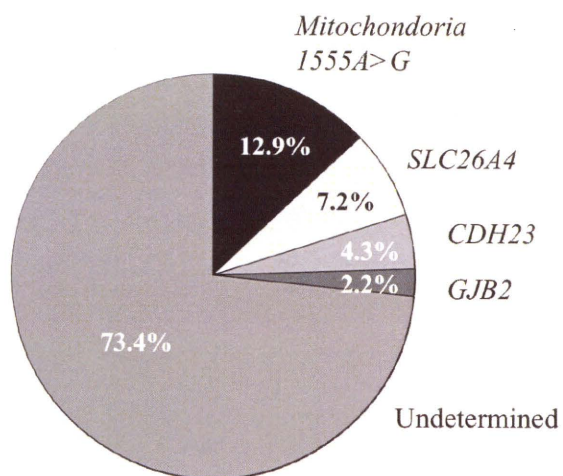


図7 難聴原因遺伝子変異の種類別に見た重ね合わせオーディオグラム

高音急墜型聴力像を呈する難聴患者を赤色でその他の難聴患者のオーディオグラムを黒色で示す。(Usami et al., 2010)

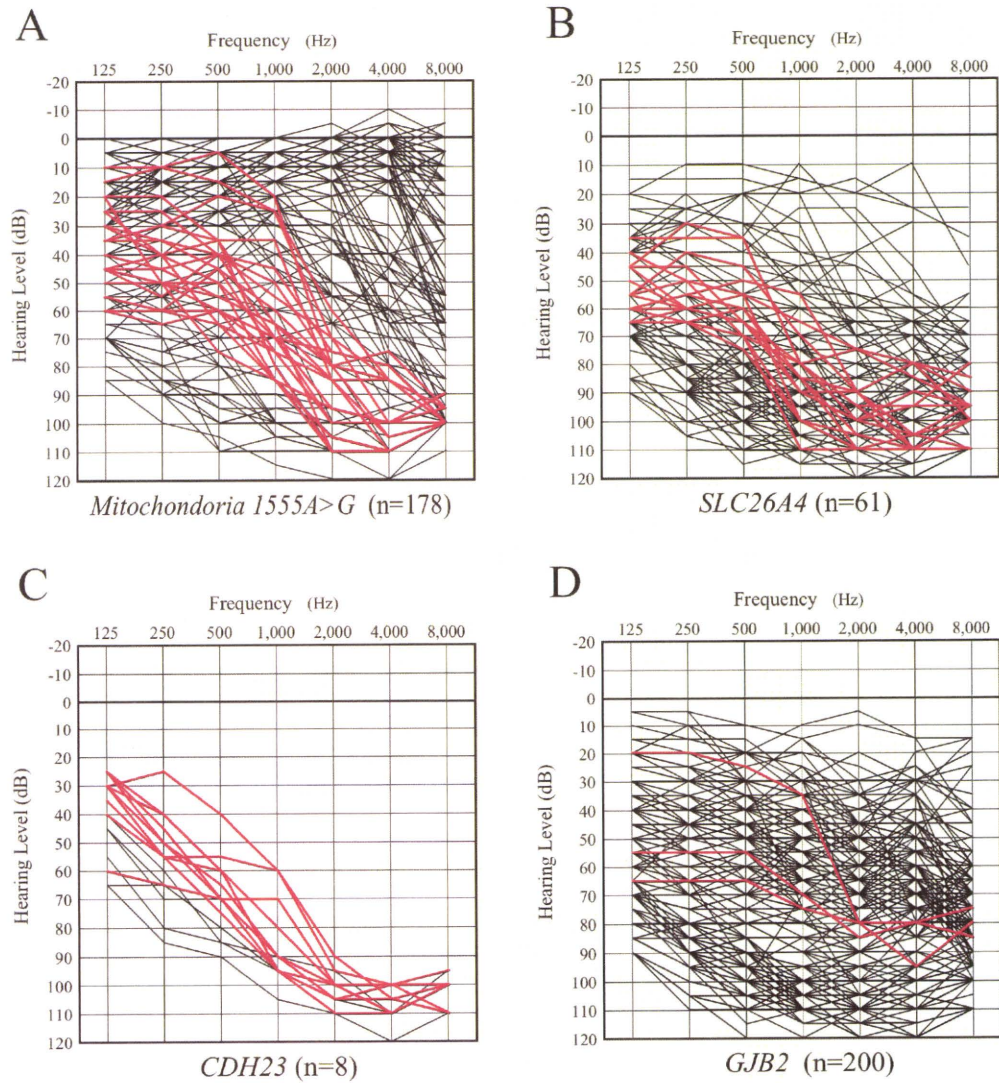


図8 日本人難聴患者 1845 例を対象に実施した、CDH23 遺伝子変異 4 種類のアリル頻度 P240L 変異、R2029W 遺伝子変異の頻度が高く、founder effect によるものであることが推定される。(Miyagawa et al., submitted)

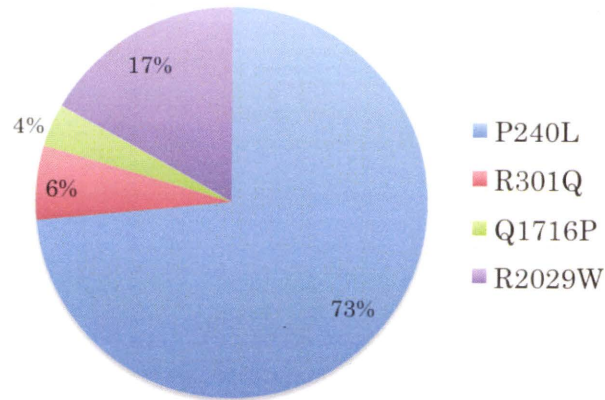


図9 保存乾燥臍帯を用いた先天性 CMV 感染症の検査の結果

1, 2, 3 はそれぞれサイトメガロウイルス上に設計した CMV_1、CMV_2、CMV_S プライマーの増幅産物、M はマーカーを示す。+ はポジティブコントロール、- はネガティブコントロールの結果を示す。(Furutate et al., submitted)

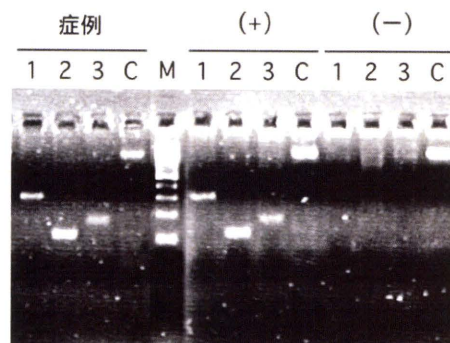


図10 期間中に先進医療「先天性難聴の遺伝子診断」を受診した患者(185例)の結果。

185例中69例(37.3%)より変異が検出された。

施設名

信州大	85例
虎の門Hsp	60例
岡山大学	12例
宮崎大学	4例
京都大学	11例
群馬大学	9例
神戸市民Hsp	3例
筑波大学	1例
北海道大学	1例
九州大学	1例
山口大学	1例
福岡大学	1例

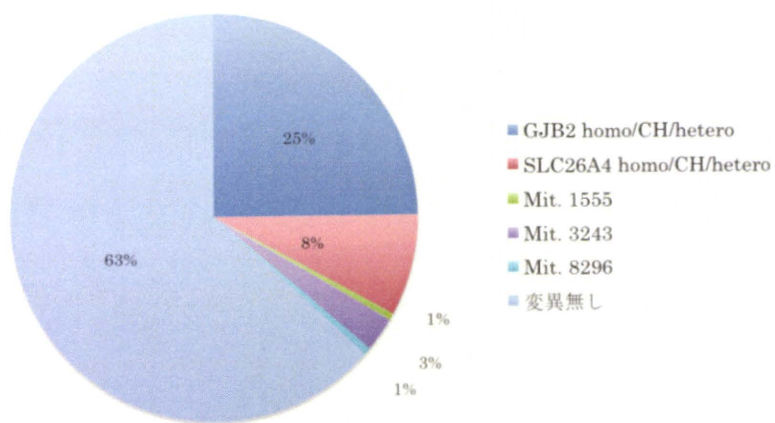


図 11 難聴の原因遺伝子変異の特定された群（特定群）とその他の群（非特定群）の WISC-III の結果の比較。動作性 IQ に関しては健聴群の平均値 100 とほぼ同等の結果であるが、言語性 IQ に関しては健聴群と比較して有為に低いことが明らかとなった。また、特定群と非特定群の比較では非特定群の方が有為に言語性 IQ の成績が低いことが示された (Maeda et al., submitted)

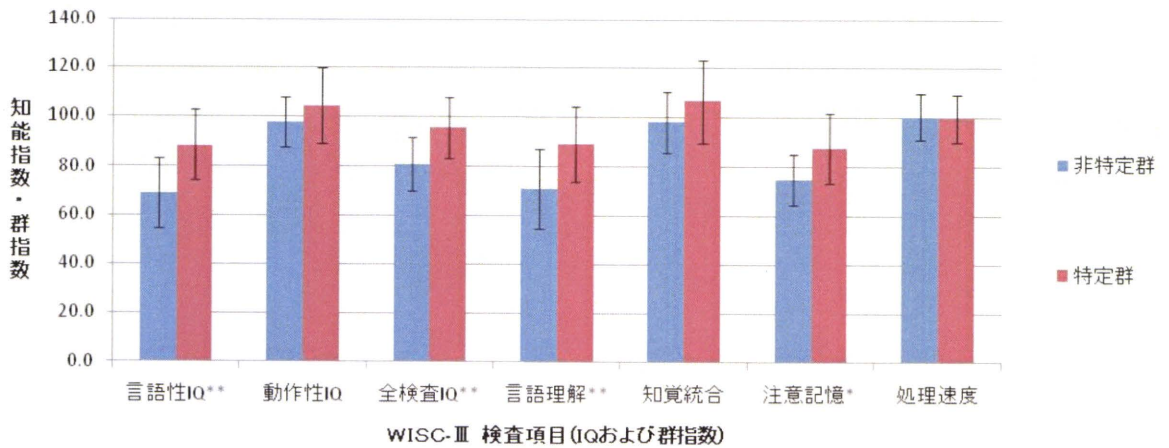
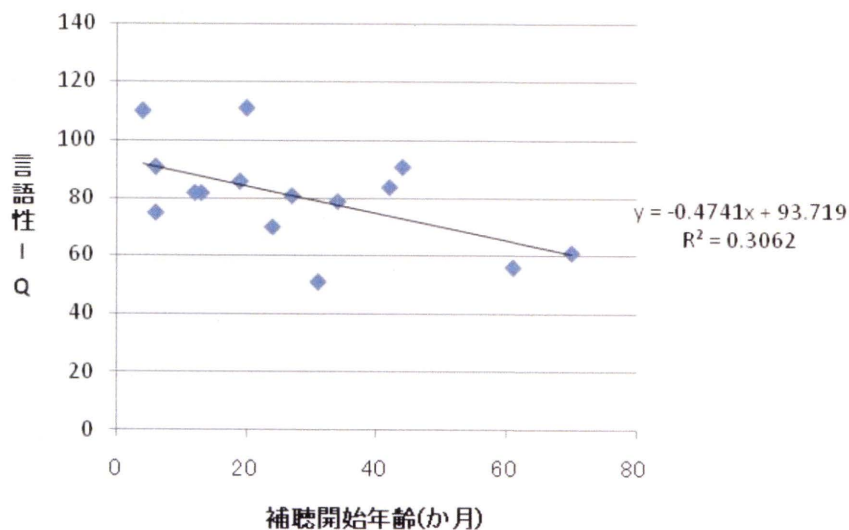


図 12 補聴器装用開始年齢と言語性 IQ の相関

装用開始年齢と言語性 IQ の間には負の相関が認められ、早期に補聴器を装用開始（早期介入開始）することで言語性 IQ の伸びをある程度担保できることが明らかとなった。



Ⅱ. 研究成果の刊行に関する一覧表

研究成果の刊行に関する一覧表

- 1) Fukuoka H, Tsukada K, Miyagawa M, Oguchi T, Takumi Y, Sugiura M, Ueda H, Kadoya M, Usami S. Quantitative evaluation of endolymphatic hydrops by bilateral intratympanic Gd-DTPA administration with MRI imaging for Meniere's disease. *Acta Oto-Laryngologica*, 2010; 130: 10-16
- 2) Miyagawa M, Fukuoka H, Tsukada K, Oguchi T, Takumi Y, Sugiura M, Ueda H, Kadoya M, Usami S. Endolymphatic hydrops and therapeutic effects are visualized in "atypical" Meniere's disease. *Acta Otolaryngol.* 2009
- 3) Lu SY, Nishio S, Tsukada K, Oguchi T, Kobayashi K, Abe S, Usami S. Factors that affect hearing level in individuals with the mitochondrial 1555A>G mutation. 2009 May;75(5):480-4.
- 4) Usami S, Takumi Y, Suzuki N, Oguchi T, Oshima A, Suzuki H, Kitoh R, Abe S, Sasaki A, Matsubara A. The localization of proteins encoded by CRYM, KIAA1199, UBA52, COL9A3, and COL9A1, genes highly expressed in the cochlea. *Neuroscience*. 2008 Jun 12;154(1):22-8.
- 5) Oshima A, Jaijo T, Aller E, Millan JM, Carney C, Usami S, Moller C, Kimberling WJ. Mutation profile of the CDH23 gene in 56 probands with Usher syndrome type I. *Hum Mutat.* 2008 Jun;29(6):E37-46.
- 6) Usami S, Wagatsuma M, Fukuoka H, Suzuki H, Tsukada K, Nishio S, Takumi Y, Abe S. The responsible genes in Japanese deafness patients and clinical application using Invader assay. *Acta Otolaryngol.* 2008 Apr;128(4):446-54.
- 7) Tsukada K, Nishio S, Usami S. A large cohort study of GJB2 mutations in Japanese hearing loss patients. *Clin. Genet.* 2010 (in press)
- 8) Usami S, Miyagawa M, Suzuki N, Moteki H, Nishio S, Takumi Y, Iwasaki S. Genetic background of candidates for EAS (electric acoustic stimulation). *Audiological Medicine*. 2010 in press.
- 9) Usami S, Moteki H, Suzuki N, Fukuoka H, Miyagawa M, Nishio S, Takumi Y, Iwasaki S, Jolly C. Achievement of hearing preservation in the presence of an electrode covering the residual hearing region. 2011. In press
- 10) Furutate S, Iwasaki S, Nishio S, Moteki H, Usami S. Clinical profile of hearing loss in children with congenital cytomegalovirus (CMV) infection: CMV DNA diagnosis using preserved umbilical cord. *Acta Oto-Laryngologica* 2011 in press.
- 11) 宇佐美真一 先天性難聴の遺伝子診断
一専門医に必要な難聴遺伝子に関する知識一 日本耳鼻咽喉科学会会報 113:34-37, 2010
- 12) 小林有美子、佐藤宏昭、岩井詔子、村井盛子、宇佐美真一 当科小児難聴外来の過去10年間における難聴の遺伝学的検討 *Audiology Japan* 53:192-198, 2010

- 13) 宇佐美真一 難聴の遺伝子診断と治療 日本医師会雑誌 139: 600-603 2010
- 14) 宇佐美 真一 疾患群の遺伝学的検査 (Genetic Testing) と遺伝子検査 (Gene-Based Testing) 日本臨床 68: 417-422 2010
- 15) 宇佐美真一 難聴の遺伝子診断 日本臨床 69: 357-365
- 16) 宇佐美真一 難聴の遺伝カウンセリング-先進医療としての「先天性難聴の遺伝子診断」をふまえて-耳鼻咽喉科臨床 2008; 101:727-738
- 17) 宇佐美真一 小児難聴児への対応-難聴遺伝子診療外来、人工内耳センター、難聴児支援センターにおけるチーム医療-耳鼻咽喉科・頭頸部外科 2008; 80:851-858
- 18) 宇佐美真一 難聴とウイルス感染 MB ENT 99:8-16, 2009
- 19) 宇佐美真一 先天性難聴 小児科 50:1182-1185, 2009
- 20) 武市紀人、柏村正明、中丸裕爾、津府久崇、福田諭、鈴木美華、宇佐美真一 難聴遺伝子診断が有用であった人工内耳一症例 Audiology Japan 52: 214-219, 2009
- 21) 宇佐美真一 薬剤と遺伝子 耳鼻咽喉科・頭頸部外科 81: 759-767 2009
- 22) 宇佐美 真一 予防医学からみた遺伝性難聴 JOHNS 25: 1719-1723 200

IV. 研究成果の刊行物・別刷

ORIGINAL ARTICLE

Semi-quantitative evaluation of endolymphatic hydrops by bilateral intratympanic gadolinium-based contrast agent (GBCA) administration with MRI for Meniere's disease

HISAKUNI FUKUOKA¹, KEITA TSUKADA¹, MAIKO MIYAGAWA¹,
TOMOHIRO OGUCHI¹, YUTAKA TAKUMI¹, MAKOTO SUGIURA²,
HITOSHI UEDA³, MASUMI KADOYA³ & SHIN-ICHI USAMI¹

¹Department of Otorhinolaryngology, Shinshu University School of Medicine, Matsumoto, ²Department of Otorhinolaryngology, Kariya Toyota General Hospital and ³Department of Radiology, Shinshu University School of Medicine, Matsumoto, Japan

Abstract

Conclusion: Bilateral intratympanic administration of a gadolinium-based contrast agent (GBCA) in MRI was successfully performed and proved to be beneficial in the semi-quantitative evaluation of endolymphatic hydrops. Such image-based diagnosis will lead to re-evaluation and reclassification of the diagnostic criteria for Meniere's disease (MD). **Objective:** To visualize endolymphatic hydrops semi-quantitatively in patients with MD, by using bilateral intratympanic GBCA administration with MRI. **Patients and methods:** A total of 13 patients were evaluated, including 12 with MD and one with acute low-tone sensorineural hearing loss. Diluted gadodiamide (a kind of GBCA) was administered to the bilateral tympanic cavity by injection through the tympanic membrane. After 24 h, the endolymphatic hydrops was evaluated with a 3.0 T MR scanner. The areas enhanced by gadodiamide were measured semi-quantitatively. **Results:** Three-dimensional, fluid-attenuated inversion recovery (3D-FLAIR) MRI showed that the gadodiamide successfully penetrated the round window membrane, entering the perilymphatic space and delineating the gadodiamide-enhanced perilymphatic and gadodiamide-negative endolymphatic spaces of the inner ear. All the patients with MD showed a reduced gadodiamide-enhanced area representing the perilymphatic space, and the quantitative ratio was 0.15 to 0.85. Furthermore, endolymphatic hydrops was also demonstrated in the patient with atypical MD who had fluctuating low frequency sensorineural hearing loss without vertigo.

Keywords: Endolymphatic hydrops, Meniere's disease, semi-quantitative analysis, gadolinium, gadolinium-based contrast agent (GBCA), MRI

Introduction

Meniere's disease (MD) is an idiopathic disorder of the inner ear characterized by fluctuating sensorineural hearing loss (SNHL), tinnitus and aural fullness, and recurrent spontaneous episodic rotational vertigo (see Sajjadi and Paparella for review [1]). MD has been thought to be attributable to endolymphatic hydrops, but this has only been confirmed histopathologically after death. Therefore, MD has been diagnosed on the basis of clinical symptoms and is classified into typical MD with all cochlear and vestibular symptoms, and atypical MD

with either cochlear symptoms (e.g. hearing loss, tinnitus, aural pressure) or vestibular symptoms (e.g. vertigo alone with aural pressure) [2]. Typical MD can further be classified into certain, definite, probable, and possible MD according to the nature of the hearing loss, tinnitus, aural fullness, and vertigo [2]. In addition, clinical diagnosis has sometimes been hampered by other conditions that closely resemble MD, such as acute low tone sensorineural hearing loss (ALSNHL) [3]. Therefore, along with clinical symptoms, clinical tests suggestive for endolymphatic hydrops are usually used for diagnosis. Functional

Correspondence: Shin-ichi Usami MD PhD, Department of Otorhinolaryngology, Shinshu University School of Medicine, 3-1-1 Asahi, Matsumoto 390-8621, Japan. Tel: +81 263 37 2666. Fax: +81 263 36 9164. E-mail: usami@shinshu-u.ac.jp

(Received 16 December 2008; accepted 16 December 2008)

ISSN 0001-6489 print/ISSN 1651-2251 online © 2010 Informa UK Ltd. (Informa Healthcare, Taylor & Francis As)
DOI: 10.3109/00016480902858881

RIGHTS LINK

testing including electrocochleography (EcochG) or glycerol test has been used to estimate endolymphatic hydrops [1]. However, even if functional testing is performed, the results are still indirect proof.

Recent advances in imaging by three-dimensional, fluid-attenuated inversion recovery (3D-FLAIR) of magnetic resonance imaging (MRI), in association with enhancement by gadolinium-based contrast agents (GBCAs), enables visualization of endolymphatic hydrops in patients with MD [4–6]. In the present study, involving patients with typical MD, atypical MD, and ALSNHL, we evaluated endolymphatic hydrops in a semi-quantitative manner, through comparison of bilateral perilymphatic spaces enhanced by a GBCA.

Patients and methods

Subjects

Ten patients with ‘definite’ MD and one with ‘possible’ MD who met the American Academy of Otolaryngology-Head and Neck Surgery (AAO-HNS) criteria, one patient with atypical MD (who had fluctuated low frequency sensorineural hearing loss without vertigo), and one patient with acute low-tone sensorineural hearing loss (ALSNHL) participated in this study.

MRI

Gadodiamide (Omniscan, Daiichi Pharmaceutical Co. Ltd, Tokyo) was diluted eightfold with saline, and 0.4–0.6 ml of the diluted gadodiamide was administered to the bilateral tympanic cavity by injection through the tympanic membrane using a 23 G needle. The injection was carried out under a microscope. The patient then lay down in the supine position for 60 min. After 24 h, the endolymphatic hydrops was evaluated by MRI. We used a 3.0 T

MR scanner (Trio, Siemens, Erlangen, Germany) with a receive-only eight-channel phased-array coil. It can perform T1-weighted three-dimensional (3D) magnetization prepared rapid gradient echo (MP-RAGE). The parameters for MP-RAGE were: TR 1500 ms, TE 3 ms, matrix size of $320 \times 290 \times 320$; 72 axial 0.8 mm thick slice, $0.8 \text{ mm} \times 0.8 \text{ mm} \times 0.8 \text{ mm}$ isotropic voxels, heavily T2-weighted 3D-TSE sequence, and 3D fluid-attenuated inversion recovery (FLAIR) with variable flip angle echo train (SPACE). The parameters for heavily T2-weighted SPACE were: TR 1350 ms, TE 199 ms, echo train length (ETL) 93, matrix size of $320 \times 288 \times 278$, 56 axial 0.8 mm thick slice, and voxel size of $0.6 \times 0.4 \times 0.8 \text{ mm}$. In addition to the methods described previously, we used 3D-FLAIR with higher in-plane spatial resolution. The scan parameters for the 3D-FLAIR sequence were as follows: repetition time of 10 000 ms, echo time of 666 ms, inversion time of 2500 ms, single slab 3D turbo spin echo with variable flip angle distribution, echo train length of 173, matrix size of 320×320 , 52 axial 0.8 mm thick slices to cover the labyrinth with a 20 cm square field of view, acceleration factor of two using the parallel imaging technique, and generalized autocalibrating partially parallel acquisitions. Voxel size was $0.7 \times 0.8 \times 0.8 \text{ mm}$. The number of excitations was one and the scan time was 9 min.

The multi-planar reconstruction (MPR) image was created from 3D-FLAIR images by imaging analysis software (Aquarius Net Viewer). The areas enhanced by gadodiamide in the cochlea and vestibule were traced and measured on the image in the plane perpendicular to the modiolus. Then, the affected side/contralateral side ratios were calculated (Figure 1). Semi-quantitative comparison of endolymphatic space in the vestibule was also calculated using Dicom Viewer software (EV Insite).

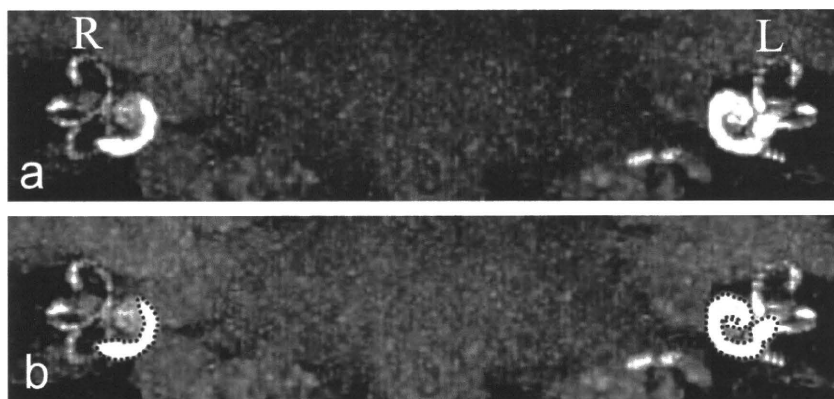


Figure 1. The areas enhanced by gadodiamide in cochlea and vestibule were measured using multi-planar reconstruction (MPR) image by imaging analysis software (dotted lines), and the affected side/unaffected side ratios were calculated.

Clinical testing

Pure tone audiometry (PTA) was performed before and after the experiment. The average of 0.5, 1, 2, and 4 Hz is shown in Table I. For vestibular testing, caloric testing and vestibular-evoked myogenic potential (VEMP) testing were performed. In caloric testing, maximum slow eye velocity was measured by cold water irrigation (20°C, 5 ml, 20 s). In VEMP testing, the electrographic signal from the stimulated side was amplified and averaged using a Neuropack evoked potential recorder (Nihon Kohden Co. Ltd, Tokyo, Japan). Clicks lasting for 0.1 ms at 105 dBnHL were presented through a headphone. The stimulation rate was 5 Hz, the band-pass filter intensity was 20–2000 Hz, and analysis time was 50 ms. The responses to 200 stimuli were averaged twice.

The Ethics Review Committee of Shinshu University School of Medicine approved the protocol of the study and all patients gave their informed consent to participation.

Results

In this study, 3D-FLAIR MRI clearly showed that the gadodiamide successfully penetrated the round window membrane, entered the perilymphatic space, and delineated the gadodiamide-enhanced perilymphatic and gadodiamide-negative endolymphatic spaces of the inner ear. The endolymphatic space is comparatively small and difficult to identify as a vacant area in the normal side. In contrast, the endolymphatic space in an ear with endolymphatic hydrops is partially or entirely expanded, making

identification of the endolymphatic space easier (Figures 2 and 3).

Gadodiamide distribution patterns within the inner ear were variable and differed individually. In patient no. 3, who had definite MD, after 24 h the intratympanic gadodiamide moved toward the perilymphatic space, and the endolymphatic hydrops could be detected as a black area surrounded by the perilymphatic space filled with the gadodiamide in the basal turn of the left cochlea (Figure 2). In the unaffected side, the endolymphatic space (which was significantly small) may have been masked by the strong enhancement of perilymphatic space. In patient no. 6, who also had definite MD, the endolymphatic space in the vestibule on the affected side was significantly larger than that on the normal side (Figure 3). In this patient, in association with the imaging, VEMP was absent, but the caloric test showed normal response.

Table I summarizes imaging results and clinical data obtained for each patient. In the cases such as no. 3 or 6 mentioned above, endolymphatic hydrops could be easily identified qualitatively. However, in some cases, it was difficult to obtain supportive imaging for endolymphatic hydrops. Therefore, the present study tried to perform semi-quantitative analysis by using the MPR image, created from 3D-FLAIR images. Based on the semi-quantitative analysis, the gadodiamide-enhanced area representing the perilymphatic space ratio was 0.14 to 3.86 (Table II). In 9 of 10 patients with definite MD the ratio was reduced, and the quantitative ratio was 0.15 to 0.85 (Table II). In the exception, patient no. 4, gadodiamide was not introduced in the perilymphatic space even on the normal side, probably due to technical failure.

Table I. Summary of bilateral intratympanic gadolinium administration.

Patient no.	Age/sex	Diagnosis	Side	Caloric test CP%	VEMP	PTA-pre (dB)		PTA-post (dB)	
						Affected side	Unaffected side	Affected side	Unaffected side
1	51/M	MD	R	7.2	Depressed	38.8	15.0	38.8	15.0
2	41/F	MD	R	51.2	–	37.5	11.3	32.5	11.3
3	42/M	MD	L	41.3	Depressed	50.0	12.5	53.8	12.5
4	42/F	MD	L	19.9	ND	33.8	12.5	32.5	10.0
5	76/F	MD	L	39	ND	46.5	30.0	40.0	27.5
6	51/F	MD	R	11.9	Absent	22.5	13.8	28.8	12.5
7	53/M	ATMD	R	–	–	58.8	13.8	47.5	13.8
8	38/M	MD	R	22.6	Depressed	20.0	6.3	28.8	5.0
9	76/M	ALSNHL	R	–	–	17.5	46.3	13.8	43.8
10	67/F	MD	L	6.9	ND	55.0	28.8	52.5	26.3
11	52/F	MD	L	6.8	ND	65.0	12.5	62.5	13.8
12	53/F	MD	L	42.3	Depressed	53.8	22.5	47.5	20.0
13	33/M	pMD	R	50.6	Normal	12.5	6.3	6.3	6.3

ALSNHL, acute low tone sensorineural hearing loss; ATMD, atypical Meniere's disease; F, female; L, left; M, male; MD, 'definite' Meniere's disease; ND, not detectable; pMD, 'possible' Meniere's disease; PTA, pure-tone audiometry; R, right.

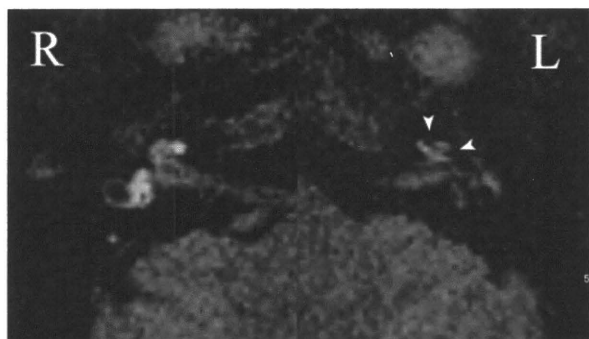


Figure 2. MRI imaging in patient no. 3 (definite Meniere's disease). The endolymphatic hydrops is detectable as a black area (arrowheads) inside the perilymphatic space filled with the gadodiamide in the basal turn of the left cochlea. In the normal side, the endolymphatic space (a significantly small area) is not detectable, probably due to strong signal intensity in the perilymphatic space.

We measured the saccular endolymphatic space by bilateral comparison. Eleven of 13 patients, including 8 with definite MD, 1 with possible MD, 1 with atypical MD, and 1 with ALSNHL, showed differences in endolymphatic space in the saccules. Significant

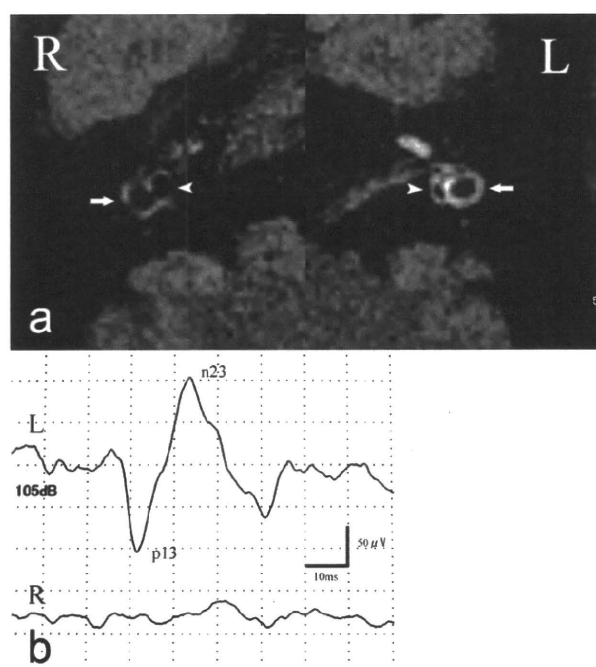


Figure 3. MRI imaging in patient no. 6 (definite Meniere's disease). The endolymphatic space in the saccules is detectable as a black area inside the perilymphatic space filled with gadodiamide in the vestibule (arrowheads). In the normal side (L), the endolymphatic space in the saccules is also detectable in the unaffected side, but is smaller than in the affected area. Arrows indicate lateral semicircular canals. In the affected side (R), enhancement by gadodiamide was weaker than in the unaffected side, indicating that endolymphatic hydrops may be present in the canal. VEMP testing showed no response in the affected side.

differences (Student's *t* test) in patient nos 6, 8, 10, and 11 were noted (Figure 4)

Concerning vestibular functional testing, caloric testing was performed in all but two patients (nos 7 and 9), and showed decreased response in five cases. VEMP testing was performed in all patients, except nos 2, 7, and 9. In 6 of the 10 patients who underwent the testing, VEMP was either absent on the affected side or depressed compared with the healthy side. VEMP amplitude could not be obtained because of low muscle contraction in patient nos 4, 5, and 10.

No adverse effects, such as vertigo, hearing deterioration, or tinnitus due to the intratympanic injection of gadodiamide were observed and there were no changes in hearing level (Table I).

Discussion

The hallmark of MD diagnosis is to prove endolymphatic hydrops, but this has been achieved only in temporal bone histopathology after death. Initial attempts to identify endolymphatic hydrops involved visualization of the Reissner membrane, and it was successfully visualized in animals [7] and human cadavers [8]. The subsequent attempts to identify endolymphatic hydrops used intratympanic GBCA administration with 1.5 T MRI to visualize the

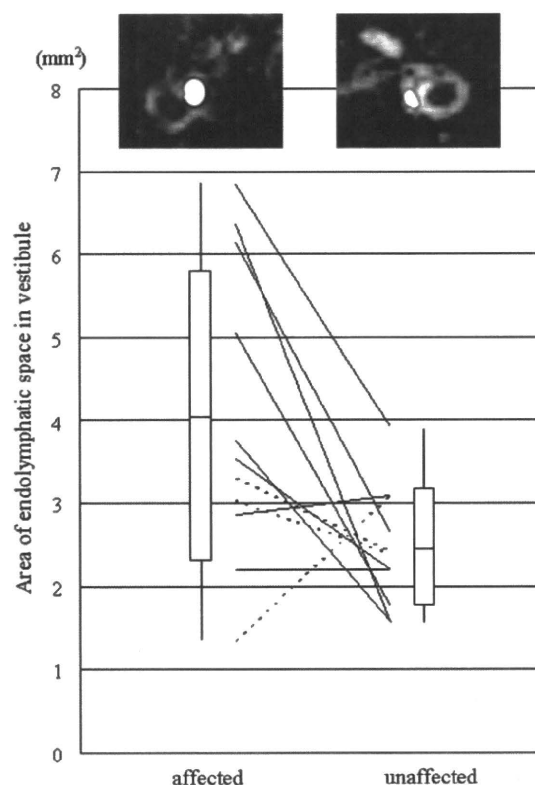


Figure 4. Semi-quantitative analysis of bilateral endolymphatic space in the sacculus.

Table II. Gadolinium distribution in inner ear.

Patient no.	Affected side			Unaffected side			Area			Area (vestibule)		
	Cochlea	Vestibule	Semicircular canals	Cochlea	Vestibule	Semicircular canals	Affected side	Unaffected side	Ratio	Affected side	Unaffected side	Ratio
1	Basal, second, apical	Whole	Whole	Basal, second, apical	Whole	Whole	17.6	26.8	0.65	2.86	3.08	
2	Basal, second, apical	Whole	Whole	Basal, second, apical	Whole	Whole	18.5	21.9	0.85	2.2	2.2	
3	Basal, second, apical	Whole	Whole	Basal, second, apical	Whole	Whole	19.6	36.8	0.53	3.74	1.57	
4	Faint	Faint	Faint	Faint	Faint	Faint	4.9	1.3	3.86	—	—	
5	Basal	Whole	Partial	Basal	Whole	Partial	15.9	19.7	0.81	—	—	
6	Faint	Faint	Partial	Basal, second	Whole	Partial	4.6	30.8	0.15	6.84	3.92	
7	Basal	Faint	Whole	Basal, second, apical	Whole	Whole	15.0	30.0	0.50	3.02	2.38	
8	Basal, second, apical	Whole	Whole	Basal, second, apical	Whole	Whole	20.4	25.6	0.80	6.37	1.54	
9	Basal, second	Whole	Whole	Basal, second, apical	Whole	Whole	26.1	27.6	0.95	3.3	2.42	
10	Basal, second, apical	Whole	Whole	Basal, second, apical	Whole	Whole	18.1	33.1	0.55	5.05	1.76	
11	Basal, second, apical	Whole	Whole	Basal, second, apical	Whole	Whole	10.7	20.1	0.53	6.15	2.64	
12	Basal, second	Faint	Whole	Basal, second, apical	Whole	Whole	5.6	25.2	0.22	3.52	2.2	
13	Basal, second, apical	Whole	Whole	Basal, second, apical	Whole	Whole	21.2	20.9	1.01	1.32	3.08	